Unconventional Spin Hall Magnetoresistance in Noncollinear Antiferromagnet/Heavy-Metal Stacks

Tomohiro Uchimura,[1,2] Jiahao Han,[1,3,*] Ping Tang,[3,†] Ju-Young Yoon,[1] Yutaro Takeuchi,[3,4] Yuta Yamane,[1,5] Shun Kanai,[1,2,3,6,7,8,9] Gerrit E. W. Bauer,[3,8,10,11] Hideo Ohno,[1,2,3,8,12] and Shunsuke Fukami[1,2,3,8,12,13,‡]

[1]*Laboratory for Nanoelectronics and Spintronics, Research Institute of Electrical Communication, Tohoku University, Sendai, Japan*
[2]*Graduate School of Engineering, Tohoku University, Sendai, Japan*
[3]*Advanced Institute for Materials Research, Tohoku University, Sendai, Japan*
[4]*International Center for Young Scientists, National Institute for Materials Science, Tsukuba, Japan*
[5]*Frontier Research Institute for Interdisciplinary Sciences, Tohoku University, Sendai, Japan*
[6]*PRESTO, Japan Science and Technology Agency, Kawaguchi, Japan*
[7]*Division for the Establishment of Frontier Sciences of Organization for Advanced Studies at Tohoku University, Tohoku University, Sendai, Japan*
[8]*Center for Science and Innovation in Spintronics, Tohoku University, Sendai, Japan*
[9]*National Institutes for Quantum Science and Technology, Takasaki, Japan*
[10]*Institute for Materials Research, Tohoku University, Sendai, Japan*
[11]*Kavli Institute for Theoretical Sciences, University of the Chinese Academy of Sciences, Beijing, China*
[12]*Center for Innovative Integrated Electronic Systems, Tohoku University, Sendai, Japan*
[13]*Inamori Research Institute for Science, Kyoto, Japan*

(Received 16 May 2024; revised 13 November 2024; accepted 24 January 2025; published 3 March 2025)

We study the spin Hall magnetoresistance (SMR) in noncollinear antiferromagnet Mn_3Sn/heavy-metal stacks. The measured SMR exhibits peculiar magnetic field angle and magnitude dependence that sharply deviates from the conventional SMR theory based on the dampinglike spin-transfer torque. An alternative model based on a coherent fieldlike torque reproduces the observations well. Our work reveals a previously unrecognized mechanism of interfacial exchange that indicates a precession of the conduction-electron spins in the collective local exchange fields of the noncollinear antiferromagnetic order. The unraveled physics is essential to understanding and controlling spin transport in unconventional magnetic materials.

DOI: 10.1103/PhysRevLett.134.096701

Antiferromagnets (AFMs) have been enthusiastically studied in spintronics due to their potential for high-efficiency, high-density, and ultrafast devices for memory and computing [1–3]. When an AFM is attached to a normal conductor with significant spin-orbit interaction, an applied charge current $\mathbf{j}_c$ in the latter can switch [4–9] or excite the antiferromagnetic order [10–12] by a spin Hall current $\mathbf{j}_s^i$ and a concomitant nonequilibrium spin accumulation $\boldsymbol{\mu}_s$ at the interface [Fig. 1(a)]. Meanwhile, a reflected spin current $\mathbf{j}_s^r$ at the interface is subsequently converted to a feedback charge current that modulates the resistance of the normal conductor. This effect is known as spin Hall magnetoresistance (SMR) [13]. Since its first observation in ferromagnets (FMs), the studies of the SMR and the related effects have advanced the understanding of spin dynamics and transport induced by the spin Hall effect [13–15], the Rashba-Edelstein effect [16], the spin-momentum locking of topological surface states [17], the orbital Hall and Rashba-Edelstein effects [18], etc., and to study the interplay between spin currents and complex magnetic textures such as antiferromagnetic orders [19–24], spiral spin structures [25], and skyrmions [26,27].

At the interface between a resistive magnet and a normal conductor with dominant exchange interaction, the SMR is determined by the spin current that flows along the perpendicular direction of the film plane and is absorbed at the interface, formulated by scattering theory as $\mathbf{j}_s = \mathbf{j}_s^i - \mathbf{j}_s^r \propto G_r \sum_\nu \mathbf{m}_\nu \times (\mathbf{m}_\nu \times \hat{\mathbf{y}}) + G_i \sum_\nu \mathbf{m}_\nu \times \hat{\mathbf{y}}$ [28,29]. The unit vectors $\{\mathbf{m}_\nu\}$ represent the set of sublattice magnetic moments with index ν and $\hat{\mathbf{y}}$ denotes the polarization of the incident spin current $\mathbf{j}_s^i$ in the coordinate system of Fig. 1(a). $G_{\uparrow\downarrow} \equiv G_r + iG_i = (e^2/\pi\hbar)\sum_{nm}(\delta_{nm} - r_{nm}^{\uparrow} r_{nm}^{\downarrow *})$ is the spin-mixing conductance in terms of the reflection amplitudes $r_{nm}^{\uparrow(\downarrow)}$ of spin-up and spin-down electrons, where $e = |e|$ is the magnitude of the electron charge and $\hbar$ is the reduced Planck constant. The real and imaginary parts of $G_{\uparrow\downarrow}$ quantify the

*Contact author: jiahao.han.c8@tohoku.ac.jp
†Contact author: tang.ping.a2@tohoku.ac.jp
‡Contact author: s-fukami@riec.tohoku.ac.jp

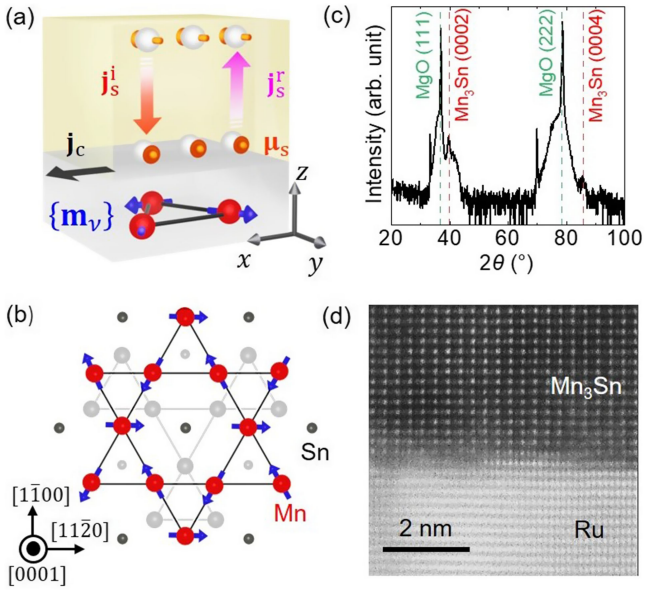

FIG. 1. Schematic of the SMR configuration and basic characterization of the sample. (a) Charge current $\mathbf{j}_c$, incident and reflected spin currents $\mathbf{j}_s^i$ and $\mathbf{j}_s^r$, and interfacial spin accumulation $\boldsymbol{\mu}_s$ in a magnet $\{\mathbf{m}_\nu\}$/heavy-metal stack. The directions of $\mathbf{j}_s^i$ and $\mathbf{j}_s^r$ are the spin polarizations of currents along z. (b) Atomic and spin structures in a kagome plane of Mn_3Sn. The shadowed atoms locate in the neighboring kagome plane. (c) Out-of-plane x-ray diffraction plot and (d) cross-section scanning transmission electron microscopy image of a Ru(5 nm)/Mn_3Sn(30 nm)/MgO(1.3 nm)/Ru(1 nm) sample on a MgO (111) single-crystal substrate, in which Mn_3Sn has a (0001) epitaxy.

contributions of individual dampinglike and fieldlike torques by the sum over $\{\mathbf{m}_\nu\}$, dissipating $\boldsymbol{\mu}_s$ and rotating it from the $\hat{\mathbf{y}}$ direction. In the conventional theory, only the G_r term contributes to the spin current component $\mathbf{j}_s^r$ parallel to $\mathbf{j}_s^i$, thereby modulating the resistivity ρ of the normal conductor in the form of a feedback charge current induced by the inverse spin Hall effect. Combining scattering with diffusion theory in the normal conductor leads to $\rho \approx \rho_0 - \Delta\rho \sum_\nu (\mathbf{m}_\nu \cdot \hat{\mathbf{y}})^2$, where ρ_0 is a constant and $\Delta\rho$ is the SMR magnitude that increases with G_r [30,31]. This picture reflects the current understanding of the SMR in FMs and AFMs [13,20–23] and shares similar physics with the spin pumping and the spin Seebeck effect [32]. In the particular case of collinear AFMs with two sublattice moments $\mathbf{m}_A = -\mathbf{m}_B$ and a Néel vector $\mathbf{n} = (\mathbf{m}_A - \mathbf{m}_B)/2$, $\mathbf{j}_s$ reduces to $G_r\mathbf{n} \times (\mathbf{n} \times \hat{\mathbf{y}})$, leading to $\rho \approx \rho_0 - \Delta\rho(\mathbf{n} \cdot \hat{\mathbf{y}})^2$ [21–23]. To first order the fieldlike torque due to G_i contributes an anomalous Hall-like effect in ferromagnetic systems [33–35]. However, it remains elusive whether the fieldlike torque can play a fundamental role in the antiferromagnetic SMR.

The recently studied noncollinear AFMs, represented by $D0_{19}$-Mn_3Sn [36], offer an intriguing platform to tackle the above questions by their unique magnetic order. Mn_3Sn exhibits an inverse-triangular chiral-spin structure containing three magnetic sublattices $\{\mathbf{m}_A, \mathbf{m}_B, \mathbf{m}_C\}$ in the (0001) kagome plane [Fig. 1(b)]. A slight canting of the sublattice moments results in a small net moment $\mathbf{m} = \mathbf{m}_A + \mathbf{m}_B + \mathbf{m}_C$. The absence of a common spin quantization axis that defines spin-up and spin-down eigenstates in such a noncollinear spin structure [37] is beyond the conventional scattering-diffusion theory for the SMR [28]. The spin structure of Mn_3Sn sources a variety of unusual phenomena, including the antiferromagnetic anomalous Hall effect [36], octupole-driven tunneling magnetoresistance [37], magnetic engineering of the electronic quantum-metric structure [38], electric manipulation of topological antiferromagnetic states [9], and characteristic chiral-spin dynamics [12,39].

Here, through a combined experimental and theoretical study, we report unexpected SMR features in Mn_3Sn/heavy-metal stacks beyond current theories. By rotating the chiral-spin structure by a magnetic field, we find that the field angle dependence of the measured SMR follows the net magnetic moment rather than that of individual sublattices. This observation sharply differs from the modeling based on the dampinglike spin-transfer torque on each sublattice, and is well reproduced by a phenomenological model based on a coherent fieldlike torque that arises from a precession of the conduction-electron spins around the collective interface exchange fields. We find here that such a process modulates the spin accumulation in the heavy metal and contributes to the SMR to second order in the fieldlike spin-mixing conductance. This model is further supported by experiments showing the dependence on the applied magnetic field strength.

We deposited stacks of Ru(5 nm)/Mn_3Sn(30 nm)/MgO(1.3 nm)/Ru(1 nm) on MgO (111) single-crystal substrates by magnetron sputtering, followed by annealing at 500 °C for 1 h. The light metal Ru serves as a buffer layer to support the epitaxial growth of (0001)-oriented (or C-plane oriented) $D0_{19}$-Mn_3Sn [40]. The out-of-plane x-ray diffraction pattern of the stack is shown in Fig. 1(c). The existence of (0002) and (0004) peaks of $D0_{19}$-Mn_3Sn confirm the (0001) epitaxy with the kagome plane lying in the film plane. The scanning transmission electron microscopy image in Fig. 1(d) visualizes the (0001) epitaxy and the single-crystal ordering. We next fabricated the AFM/heavy-metal stacks of Ru(5 nm)/Mn_3Sn(15 nm)/Pt(5 nm) (Mn_3Sn/Pt in short) by etching Mn_3Sn(15 nm)/MgO/Ru and sputter-depositing Pt at room temperature without breaking the vacuum. This protocol prevents the formation of secondary phases such as a ferromagnetic MnPt alloy at the Mn_3Sn/Pt interface: see Sec. 1 of Supplemental Material [41] (SM). A control sample of Ru(5 nm)/Mn_3Sn(15 nm)/MgO(1.3 nm)/Ru(1 nm) (Mn_3Sn/MgO in short) was prepared by the same route as the Pt-capped sample, i.e., etching Mn_3Sn(15 nm)/MgO/Ru and sputter-depositing MgO/Ru at room temperature, which minimizes differences due

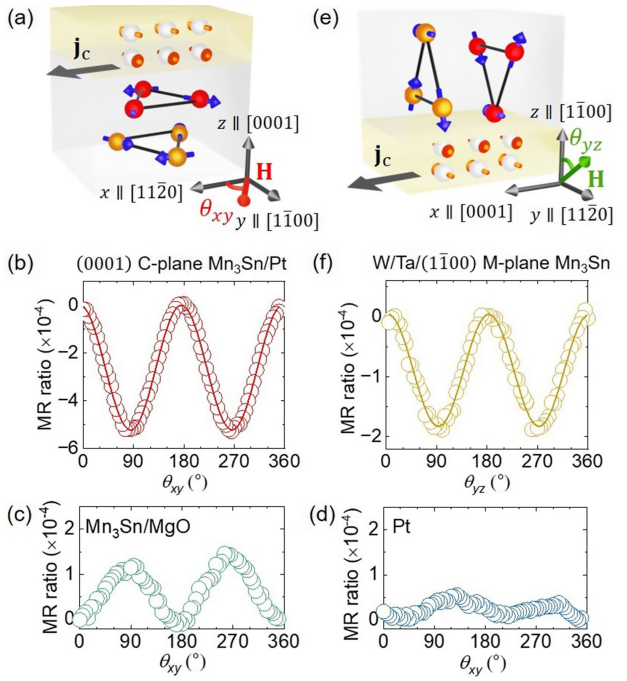

FIG. 2. Measured SMR in the Mn_3Sn/heavy-metal samples. (a) Schematic of the (0001)-oriented Mn_3Sn/Pt sample with a charge current along $x \parallel [11\bar{2}0]$ and a magnetic field $\mathbf{H}$ in the xy plane. (b)–(d) MR ratio measured in the samples of Mn_3Sn/Pt, Mn_3Sn/MgO, and just Pt in the configuration of (a). (e) Schematic of the W/Ta/($\bar{1}100$)-oriented Mn_3Sn sample with a charge current along $x \parallel [0001]$ and a magnetic field $\mathbf{H}$ in the yz plane. (f) MR ratio measured in the sample of (e). The lines in (b) and (f) are fits to $-\sin^2\theta_{xy,yz}$. The magnetic field is kept at 9 T in this figure.

to etching with the main experiment. We carried out measurements at room temperature unless specified.

The magnetic hysteresis loops of Mn_3Sn/Pt in SM Sec. 1 [41] show a coercivity < 30 mT and a weak net magnetization of 18 mT at the alignment field of 0.5 T, as observed in previous studies on Mn_3Sn thin films with the same orientation [48]. An applied field in the kagome plane of several teslas therefore fully rotates the chiral-spin structure. Moreover, nearly identical hysteresis loops after zero-field and field cooling protocols are consistent with the absence of secondary ferromagnetic phases at the Mn_3Sn/Pt interface.

Figure 2(a) depicts the scheme for measuring the longitudinal resistance R of Mn_3Sn/Pt in a patterned stripe device with a rotating magnetic field $\mathbf{H}$ of 9 T in the kagome plane. The magnetic field is strong enough to fully rotate the chiral-spin structure and make $\mathbf{m} \parallel \mathbf{H}$. The magnetoresistance (MR) ratio $[R(\theta_{xy}) - R(0°)]/R(0°)$ is negative and reaches a peak value of -5×10^{-4} (or 0) when $\mathbf{m}$ is parallel (or perpendicular) to the electron spin [Fig. 2(b)]. This trend is inconsistent with reports on the SMR of collinear AFM/Pt bilayers, but agrees with the phenomenology of the conventional SMR in FM/Pt. We argue that it should not be attributed to an extra ferromagnetic order of Mn_3Sn, if any. The first reason is that the angle-dependent MR of Mn_3Sn/MgO without Pt capping [Fig. 2(c)] strongly differs from the MR of Mn_3Sn/Pt and the anisotropic magnetoresistance (AMR) of a ferromagnetic order. Instead, it is consistent with the chiral anomaly-induced transport in the Weyl semimetal states [9,47]. To the best of our knowledge, ferromagnetic phases hardly occur at the surface or interfaces of high-quality Mn_3Sn, as indicated in SM Sec. 1 [41]. The second reason is that the MR ratio keeps increasing with the magnetic field up to 9 T (to be shown later in Fig. 4), while a hypothetical residual ferromagnetic phase and its induced MR should saturate at a moderate field [49]. The ordinary MR in a Pt sample without Mn_3Sn is very small [Fig. 2(d)]. These observations are consistent with earlier MR measurements in Mn_3Sn-based heterostructures in terms of magnitude and angle dependence [50,51]. Moving forward, this study will reveal unique features and origins of the spin transport subject to the noncollinear antiferromagnetic order, to be demonstrated in Figs. 3 and 4.

In FM/Pt, an interfacial proximity effect may contribute to the AMR by magnetizing the Pt atoms at the interface [52]. A common approach to assess such contribution is to rotate the magnetization in the orthogonal planes of xy, yz, and zx. As a key feature, the SMR (AMR) should dominate (disappear) in the yz scan, as the angle between the electron spin (charge current) and the magnetization varies (does not change) [13,53]. We perform the yz scan in a ($1\bar{1}00$)-oriented (or M-plane oriented) Mn_3Sn sample grown on heavy-metal W/Ta buffer layers, MgO (110) substrate/W(2 nm)/Ta(3 nm)/Mn_3Sn(15 nm)/MgO (1.3 nm)/Ru(1 nm) in detail (the epitaxial growth follows the methods in Refs. [12,40]), where the kagome lattice lies in the yz plane so that the magnetic field can fully rotate the chiral-spin structure [39] [Fig. 2(e)]. The measured MR in Fig. 2(f) shows the same trend as that in Fig. 2(b), which supports the SMR mechanism. The SMR decreases with the thickness of Mn_3Sn, which can be explained by the shunting of the current in the W/Ta heavy-metal layers by the metallic AFM (SM Sec. 2 [41]). Furthermore, given that the magnetization of Mn_3Sn is much smaller than that of the ferrimagnetic $Y_3Fe_5O_{12}$ and the ferromagnetic Co, the proximity-induced AMR is unlikely to contribute by $> 10^{-5}$ to the total MR ratio of Mn_3Sn/Pt. Thus, we attribute the observed MR in the (0001) and ($1\bar{1}00$)-oriented Mn_3Sn/heavy-metal samples to the SMR. The unequal SMR magnitudes of these samples should be due to the different heavy metals, interfacial structures, and magnetic orientations. The angle-dependent MR with all rotational planes of (0001) and ($1\bar{1}00$)-oriented Mn_3Sn/heavy-metal samples in SM Sec. 3 [41] confirms our SMR scenario.

We now move on to explain the origin of the observed exceptional SMR for the noncollinear AFM Mn_3Sn.

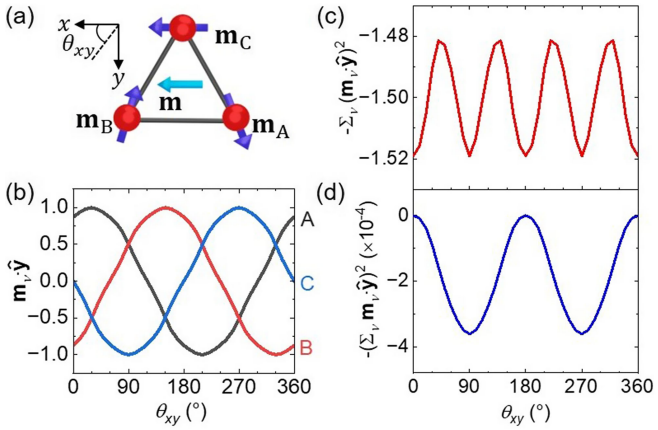

FIG. 3. Calculated orientations of the sublattice magnetic moments $\{\mathbf{m}_\nu\}(\nu = \mathrm{A}, \mathrm{B}, \mathrm{C})$ in Mn_3Sn. (a) Orientations of $(\mathbf{m}_\nu)$ and the net magnetic moment $\mathbf{m}$ under a magnetic field of 9 T along x. The canting of $\mathbf{m}_\mathrm{A}$ and $\mathbf{m}_\mathrm{B}$ from the edges of an equilateral triangle is exaggerated for a clear view. (b) y component of $\{\mathbf{m}_\nu\}$, (c) $[-\sum_\nu (\mathbf{m}_\nu \cdot \hat{\mathbf{y}})^2]$, and (d) $[-(\sum_\nu \mathbf{m}_\nu \cdot \hat{\mathbf{y}})^2]$ as a function of the magnetic field angle.

We start with calculating the orientations of the unit vectors $\{\mathbf{m}_{\nu(\mu)}\}$ $(\mu, \nu = \mathrm{A}, \mathrm{B}, \mathrm{C})$ [Fig. 3(a)] by minimizing the magnetic free energy density $u = J_0 \sum_{\mu,\nu} \mathbf{m}_\mu \cdot \mathbf{m}_\nu - D_0 \hat{\mathbf{z}} \cdot \sum_{\mu,\nu} \mathbf{m}_\mu \times \mathbf{m}_\nu - K \sum_\nu (\mathbf{m}_\nu \cdot \mathbf{e}_\nu)^2 - M_\mathrm{s} \mathbf{H} \cdot \sum_\nu \mathbf{m}_\nu$, with exchange constant $J_0 = 2 \times 10^8$ Jm^{-3}, bulk Dzyaloshinskii-Moriya interaction constant $D_0 = 10^7$ Jm^{-3}, anisotropy constant $K = 2 \times 10^6$ Jm^{-3}, spontaneous magnetization of one magnetic sublattice $M_\mathrm{s} = 0.3$ T, and unit vector $\mathbf{e}_\nu$ connecting two Sn atoms as the closest neighbors of a Mn atom, which gives rise to the sixfold anisotropy [54]. Figure 3(b) plots the y component of $\{\mathbf{m}_\nu\}$ as a function of the angle of a 9 T in-plane magnetic field. We first calculate the angle dependence of the SMR in the conventional formula of $(\rho - \rho_0)/\Delta\rho \approx -\sum_\nu (\mathbf{m}_\nu \cdot \hat{\mathbf{y}})^2$ [Fig. 3(c)], where each $\mathbf{m}_\nu$ interacts individually with the electron spin through the dampinglike transfer of spin angular momentum. However, it fails to reproduce the measured result in Fig. 2(b). On the other hand, the plot $(\rho - \rho_0)/\Delta\rho \approx -(\sum_\nu \mathbf{m}_\nu \cdot \hat{\mathbf{y}})^2$ in Fig. 3(d) agrees well with the observations, suggesting the emergence of a predominantly fieldlike torque. This calculation disregards the interfacial Dzyaloshinskii-Moriya interaction from Pt and the resultant out-of-kagome-plane magnetic moments that alternate among Mn atoms and are further suppressed by the large applied field, negligibly influencing the main trend of the net moment of Mn_3Sn. Given the finite SMR of W/Ta/$(1\bar{1}00)$-oriented Mn_3Sn in which such tilting vanishes, this approximation should not affect our interpretation of the SMR.

Next we show that noncollinear spin-diffusion theory explains the unconventional SMR in terms of the emergence of a fieldlike torque. The spin current generated by the spin Hall effect of Pt (with thickness d) establishes a nonuniform spin density $\mathbf{s}$ along the thickness (z) direction and

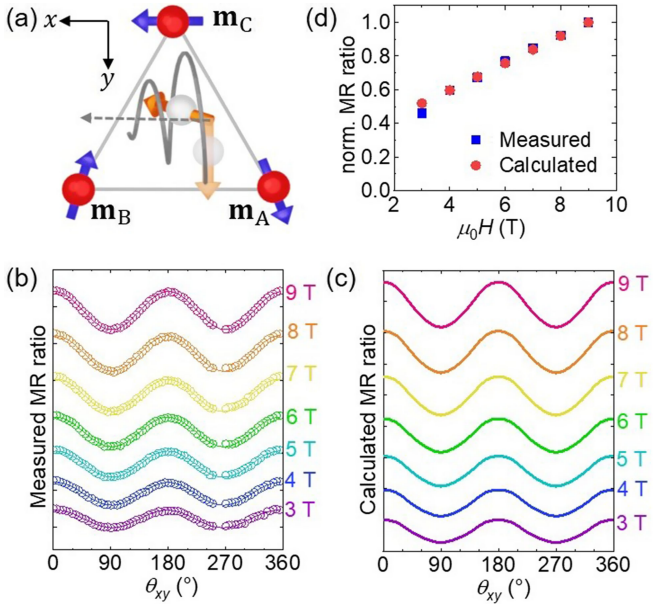

FIG. 4. Origin of the unconventional SMR. (a) Precession of conduction-electron spin due to the collective local exchange fields of the chiral-spin structure. The incident spin polarization is along y. (b) Measured MR and (c) calculated MR [SMR of Eq. (2)] in the (0001)-oriented Mn_3Sn/Pt sample at different magnetic field strengths. The lines in (b) are fits to $-\sin^2\theta_{xy}$. (d) Comparison of the measured and calculated MR magnitudes (absolute values). The data are normalized by the values at 9 T.

experiences a torque $\mathbf{T}_\mathrm{s}$ by the three sublattice moments at the Mn_3Sn/Pt interface ($z = 0$). The stationary-state spin continuity equation in Pt reads $\partial_z \mathbf{j}_\mathrm{s} = -(\mathbf{s}/\tau_\mathrm{sf}) + \mathbf{T}_\mathrm{s}$. We take $\mathbf{s} = (\hbar/2) N_\mathrm{F} \boldsymbol{\mu}_s$, with N_F the density of states per unit volume at the Fermi level and $\boldsymbol{\mu}_\mathrm{s}$ the spin chemical potential. $\mathbf{j}_\mathrm{s} = (\hbar/2e)[-(1/e\rho_0)\partial_z \boldsymbol{\mu}_\mathrm{s} + (\theta_\mathrm{SH} E/\rho_0)\hat{\mathbf{y}}]$ is the spin current density that varies along z, with ρ_0 and θ_SH the ordinary resistivity and the spin Hall angle of Pt, and E the applied electric field along x. τ_sf is the spin relaxation time [28].

The interfacial s-d exchange interaction from the chiral-spin structure of Mn_3Sn precesses the electron spin [Fig. 4(a)] by the torque

$$\mathbf{T}_\mathrm{s} = \frac{J_{sd}}{\hbar} \delta(z) \sum_\nu \mathbf{s} \times \mathbf{m}_\nu, \tag{1}$$

where J_{sd} is the interfacial s-d exchange integral in units of eVm and the delta function $\delta(z)$ indicates the interfacial torque that persists over a spatial scale of the spin dephasing length [55]. While Eq. (1) has the same form as the fieldlike torque in the existing scattering theory, calculating the rotation of $\mathbf{s}$ from the incident spin polarization $\hat{\mathbf{y}}$ poses a self-consistency problem that has been overlooked in the conventional scattering-diffusion theory for the SMR. The summation in Eq. (1) implies that the electron spin precession is a collective consequence of the local exchange fields: the torque arises coherently

from the chiral-spin structure. With boundary conditions $\mathbf{j}_s(0^+) = (J_{sd}/\hbar)\sum_\nu \mathbf{s}(0^+) \times \mathbf{m}_\nu$ and $\mathbf{j}_s(d) = 0$, we calculate $\boldsymbol{\mu}_s$ and its feedback charge current density $\delta j_c = -(\theta_{SH}/d)\int_0^d dz(1/e\rho_0)\partial_z(\boldsymbol{\mu}_s \cdot \hat{\mathbf{y}})$ in the electric field direction (x) through the inverse spin Hall effect. Accordingly, the total resistivity is given by (see derivations in SM Sec. 4 [41])

$$\rho \approx \rho_0 - \frac{\rho_0 \lambda \theta_{SH}^2}{d} \frac{\xi^2}{1+\xi^2} (\hat{\mathbf{m}} \cdot \hat{\mathbf{y}})^2, \tag{2}$$

where λ is the spin diffusion length of Pt, $\xi = (2e^2/\hbar)\rho_0 \lambda_{SF} \tilde{G}_i$ is a dimensionless parameter, and $\tilde{G}_i = \frac{1}{2} J_{sd} N_F |\mathbf{m}|$ is a fieldlike spin-mixing conductance. Equation (2) has been simplified from the general expression in SM Sec. 4 for $d \gg \lambda_{SF}$ [41]. It reflects the second-order contribution in $\tilde{G}_i$ and reproduces the angle-dependent SMR of the noncollinear AFM. Taking $\rho_0 = 30\ \mu\Omega\,\mathrm{cm}$, $\theta_{SH} = 0.12$, $\lambda = 2$ nm [49], and the measured SMR ratio of -1.1×10^{-3} that solely counts the relative resistance change of Pt [deduced from Figs. 2(b) and 2(c), after considering the current shunting and the opposite MR in Ru/Mn_3Sn], we arrive at $\xi = 0.5$ and $\tilde{G}_i = 1.7 \times 10^{18}\ \mathrm{m}^{-2}$ at 9 T, which is comparable to the real-part spin-mixing conductance in FMs and collinear AFMs [13,49,56] (for a direct comparison, one needs to multiply $\tilde{G}_i$ by $(2e^2/\hbar)$). Differences with the full version of Eq. (2) [41] do not significantly influence the magnitudes determined here.

Our $\tilde{G}_i$ is proportional to $|\mathbf{m}|$ that measures the distortion from the perfect inverse-triangular chiral-spin structure with zero net moment. In FMs and collinear AFMs, the orientation of a unit-vector magnetization or Néel vector is sufficient to determine the SMR from the dampinglike torque [22,49]. In contrast, the perfect chiral-spin structure cancels the effect of a fieldlike torque on the electron spin. Hence, observing the angle-dependent SMR in our system requires a finite $|\mathbf{m}|$, which is encoded in $\tilde{G}_i$. To verify this hypothesis, we measure the MR in Mn_3Sn/Pt with a rotating magnetic field from 3 to 9 T and find that the MR magnitude indeed increases with field strength [Fig. 4(b)]. By substituting the calculated orientations of $\{\mathbf{m}_\nu\}$ for different field strengths into Eq. (2) for the SMR [Fig. 4(c)] and considering the field-dependent chiral anomaly in the full stack (SM Sec. 5 [41]), the agreement of experiments and calculations in Fig. 4(d) supports our model and interpretation. Using the values of $\tilde{G}_i$ and $|\mathbf{m}|$ and $N_F = 10^{29}\ (\mathrm{eV})^{-1}\ \mathrm{m}^{-3}$ for Pt, we obtain $J_{sd} = 1.7 \times 10^{-9}$ eV m, matching the interface exchange constant of FM/normal metal stacks that can be estimated as the product of the exchange splitting and the spin dephasing length of the FM layer [55]. Our observations should not be attributed to the recently reported small paramagnetic SMR of -10^{-5} at low temperatures [57] that does not reflect the antiferromagnetic order essential to obtain the agreement in Fig. 4(d). The low-temperature MR in the chiral-spin phase of Mn_3Sn can be explained by our SMR model (SM Sec. 6 [41]).

One may ask why the current-induced manipulation of noncollinear AFMs is well described by the dampinglike torque even without considering the fieldlike torque. From previous works [12,54] we know that the fieldlike torque for a typical threshold current density of $10^7\ \mathrm{A/cm^2}$ is too weak to overcome the coercivity of Mn_3Sn. In contrast, the dampinglike torque from the perpendicular-to-kagome-plane component of $\mathbf{s}$ triggers the internal exchange interaction of Mn_3Sn, which is strong enough to rotate the chiral-spin structure. But why is fieldlike spin-mixing conductance in Mn_3Sn 2 orders of magnitude larger than that of FMs, either calculated [58] or measured in terms of an interface-induced anomalous Hall-like effect [35]? In wave-vector $\mathbf{k}$ resolved calculation $|G_i(\mathbf{k})|$ approximates $G_r(\mathbf{k})$, but G_i has both signs, leading to an effective cancellation when integrating over the complicated Fermi surface of transition-metal FMs [35]. Here, the spins of all electrons scattered at the interface appear to precess in an effective magnetic field of the same sign, which could be confirmed by first-principles calculations or dedicated measurements of the anomalous Hall effect.

In summary, by comparing experiments and modeling, we reveal and interpret an unconventional SMR in noncollinear AFM Mn_3Sn/heavy-metal stacks. The SMR can be explained by an interfacial fieldlike torque, which arises from the conduction-electron spin precession around the collective local exchange fields of the chiral-spin structure and thus modulates the spin current that causes the SMR in conjunction with the spin Hall effects. This mechanism opens possibilities of manipulating the antiferromagnetic spin transport by engineering the interfacial exchange interaction specific to the magnetic material, which paves a way for controlling the functionalities of AFM-based spintronics devices.

Acknowledgments—This work is partly supported by JSPS Kakenhi (No. 19H05622, No. 21J23061, No. 22KF0035, No. 22K14558, No. 23KJ0216, No. 24H00039, No. 24H02235, and No. 24K16999), JST-ASPIRE JPMJAP2322, JST TI-FRIS, Casio Science and Technology Foundation (No. 40-4), RIEC Cooperative Research Projects, and AIMR Fusion Research Projects. T. U. acknowledges support from GP-Spin of Tohoku University.

[1] T. Jungwirth, X. Marti, P. Wadley, and J. Wunderlich, Antiferromagnetic spintronics, Nat. Nanotechnol. **11**, 231 (2016).

[2] V. Baltz, A. Manchon, M. Tsoi, T. Moriyama, T. Ono, and Y. Tserkovnyak, Antiferromagnetic spintronics, Rev. Mod. Phys. **90**, 015005 (2018).

[3] J. Han, R. Cheng, L. Liu, H. Ohno, and S. Fukami, Coherent antiferromagnetic spintronics, Nat. Mater. **22**, 684 (2023).

[4] X. Z. Chen, R. Zarzuela, J. Zhang, C. Song, X. F. Zhou, G. Y. Shi, F. Li, H. A. Zhou, W. J. Jiang, F. Pan, and Y. Tserkovnyak, Antidamping-torque-induced switching in biaxial antiferromagnetic insulators, Phys. Rev. Lett. **120**, 207204 (2018).

[5] T. Moriyama, K. Oda, T. Ohkochi, M. Kimata, and T. Ono, Spin torque control of antiferromagnetic moments in NiO, Sci. Rep. **8**, 14167 (2018).

[6] S. DuttaGupta, A. Kurenkov, O. A. Tretiakov, G. Krishnaswamy, G. Sala, V. Krizakova, F. Maccherozzi, S. S. Dhesi, P. Gambardella, S. Fukami, and H. Ohno, Spin-orbit torque switching of an antiferromagnetic metallic heterostructure, Nat. Commun. **11**, 5715 (2020).

[7] Y. Cheng, S. Yu, M. Zhu, J. Hwang, and F. Yang, Electrical switching of tristate antiferromagnetic Néel order in α-Fe_2O_3 epitaxial films, Phys. Rev. Lett. **124**, 027202 (2020).

[8] P. Zhang, C.-T. Chou, H. Yun, B. C. McGoldrick, J. T. Hou, K. A. Mkhoyan, and L. Liu, Control of Néel vector with spin-orbit torques in an antiferromagnetic insulator with tilted easy plane, Phys. Rev. Lett. **129**, 017203 (2022).

[9] H. Tsai, T. Higo, K. Kondou, T. Nomoto, A. Sakai, A. Kobayashi, T. Nakano, K. Yakushiji, R. Arita, S. Miwa, Y. Otani, and S. Nakatsuji, Electrical manipulation of a topological antiferromagnetic state, Nature (London) **580**, 608 (2020).

[10] R. Lebrun, A. Ross, S. A. Bender, A. Qaiumzadeh, L. Baldrati, J. Cramer, A. Brataas, R. A. Duine, and M. Kläui, Tunable long-distance spin transport in a crystalline antiferromagnetic iron oxide, Nature (London) **561**, 222 (2018).

[11] J. Han, P. Zhang, Z. Bi, Y. Fan, T. S. Safi, J. Xiang, J. Finley, L. Fu, R. Cheng, and L. Liu, Birefringence-like spin transport via linearly polarized antiferromagnetic magnons, Nat. Nanotechnol. **15**, 563 (2020).

[12] Y. Takeuchi, Y. Yamane, J.-Y. Yoon, R. Itoh, B. Jinnai, S. Kanai, J. Ieda, S. Fukami, and H. Ohno, Chiral-spin rotation of non-collinear antiferromagnet by spin–orbit torque, Nat. Mater. **20**, 1364 (2021).

[13] H. Nakayama, M. Althammer, Y.-T. Chen, K. Uchida, Y. Kajiwara, D. Kikuchi, T. Ohtani, S. Geprägs, M. Opel, S. Takahashi, R. Gross, G. E. W. Bauer, S. T. B. Goennenwein, and E. Saitoh, Spin Hall magnetoresistance induced by a nonequilibrium proximity effect, Phys. Rev. Lett. **110**, 206601 (2013).

[14] J. Kim, P. Sheng, S. Takahashi, S. Mitani, and M. Hayashi, Spin Hall magnetoresistance in metallic bilayers, Phys. Rev. Lett. **116**, 097201 (2016).

[15] J. Sklenar, W. Zhang, M. B. Jungfleisch, W. Jiang, H. Chang, J. E. Pearson, M. Wu, J. B. Ketterson, and A. Hoffmann, Driving and detecting ferromagnetic resonance in insulators with the spin Hall effect, Phys. Rev. B **92**, 174406 (2015).

[16] H. Nakayama, Y. Kanno, H. An, T. Tashiro, S. Haku, A. Nomura, and K. Ando, Rashba-Edelstein magnetoresistance in metallic heterostructures, Phys. Rev. Lett. **117**, 116602 (2016).

[17] X. Chen, H. Bai, Y. Ji, Y. Zhou, L. Liao, Y. You, W. Zhu, Q. Wang, L. Han, X. Liu, A. Li, X. Han, J. Yin, X. Kou, F. Pan, and C. Song, Control of spin current and antiferromagnetic moments via topological surface state, Nat. Electron. **5**, 574 (2022).

[18] S. Ding, A. Ross, D. Go, L. Baldrati, Z. Ren, F. Freimuth, S. Becker, F. Kammerbauer, J. Yang, G. Jakob, Y. Mokrousov, and M. Kläui, Harnessing orbital-to-spin conversion of interfacial orbital currents for efficient spin-orbit torques, Phys. Rev. Lett. **125**, 177201 (2020).

[19] J. H. Han, C. Song, F. Li, Y. Y. Wang, G. Y. Wang, Q. H. Yang, and F. Pan, Antiferromagnet-controlled spin current transport in $SrMnO_3$/Pt hybrids, Phys. Rev. B **90**, 144431 (2014).

[20] W. Lin and C. L. Chien, Electrical detection of spin backflow from an antiferromagnetic insulator/$Y_3Fe_5O_{12}$ interface, Phys. Rev. Lett. **118**, 067202 (2017).

[21] D. Hou, Z. Qiu, J. Barker, K. Sato, K. Yamamoto, S. Vélez, J. M. Gomez-Perez, L. E. Hueso, F. Casanova, and E. Saitoh, Tunable sign change of spin Hall magnetoresistance in Pt/NiO/YIG structures, Phys. Rev. Lett. **118**, 147202 (2017).

[22] G. R. Hoogeboom, A. Aqeel, T. Kuschel, T. T. M. Palstra, and B. J. Van Wees, Negative spin Hall magnetoresistance of Pt on the bulk easy-plane antiferromagnet NiO, Appl. Phys. Lett. **111**, 052409 (2017).

[23] R. Lebrun, A. Ross, O. Gomonay, S. A. Bender, L. Baldrati, F. Kronast, A. Qaiumzadeh, J. Sinova, A. Brataas, R. A. Duine, and M. Kläui, Anisotropies and magnetic phase transitions in insulating antiferromagnets determined by a spin-Hall magnetoresistance probe, Commun. Phys. **2**, 50 (2019).

[24] E. Cogulu, H. Zhang, N. N. Statuto, Y. Cheng, F. Yang, R. Cheng, and A. D. Kent, Quantifying spin-orbit torques in antiferromagnet–heavy-metal heterostructures, Phys. Rev. Lett. **128**, 247204 (2022).

[25] A. Aqeel, N. Vlietstra, A. Roy, M. Mostovoy, B. J. van Wees, and T. T. M. Palstra, Electrical detection of spiral spin structures in Pt|Cu_2OSeO_3 heterostructures, Phys. Rev. B **94**, 134418 (2016).

[26] Q. Shao, Y. Liu, G. Yu, S. K. Kim, X. Che, C. Tang, Q. L. He, Y. Tserkovnyak, J. Shi, and K. L. Wang, Topological Hall effect at above room temperature in heterostructures composed of a magnetic insulator and a heavy metal, Nat. Electron. **2**, 182 (2019).

[27] M. Grelier, F. Godel, A. Vecchiola, S. Collin, K. Bouzehouane, A. Fert, V. Cros, and N. Reyren, Three-dimensional skyrmionic cocoons in magnetic multilayers, Nat. Commun. **13**, 6843 (2022).

[28] Y.-T. Chen, S. Takahashi, H. Nakayama, M. Althammer, S. T. B. Goennenwein, E. Saitoh, and G. E. W. Bauer, Theory of spin Hall magnetoresistance, Phys. Rev. B **87**, 144411 (2013).

[29] A. Manchon, J. Železný, I. M. Miron, T. Jungwirth, J. Sinova, A. Thiaville, K. Garello, and P. Gambardella, Current-induced spin-orbit torques in ferromagnetic and antiferromagnetic systems, Rev. Mod. Phys. **91**, 035004 (2019).

[30] K. Ganzhorn, J. Barker, R. Schlitz, B. A. Piot, K. Ollefs, F. Guillou, F. Wilhelm, A. Rogalev, M. Opel, M. Althammer, S. Geprägs, H. Huebl, R. Gross, G. E. W. Bauer, and S. T. B. Goennenwein, Spin Hall magnetoresistance in a canted ferrimagnet, Phys. Rev. B **94**, 094401 (2016).

[31] J. Fischer, O. Gomonay, R. Schlitz, K. Ganzhorn, N. Vlietstra, M. Althammer, H. Huebl, M. Opel, R. Gross, S. T. B. Goennenwein, and S. Geprägs, Spin Hall magnetoresistance in antiferromagnet/heavy-metal heterostructures, Phys. Rev. B **97**, 014417 (2018).

[32] M. Weiler, M. Althammer, M. Schreier, J. Lotze, M. Pernpeintner, S. Meyer, H. Huebl, R. Gross, A. Kamra, J. Xiao, Y.-T. Chen, H. J. Jiao, G. E. W. Bauer, and S. T. B. Goennenwein, Experimental test of the spin mixing interface conductivity concept, Phys. Rev. Lett. **111**, 176601 (2013).

[33] C. O. Avci, A. Quindeau, C.-F. Pai, M. Mann, L. Caretta, A. S. Tang, M. C. Onbasli, C. A. Ross, and G. S. D. Beach, Current-induced switching in a magnetic insulator, Nat. Mater. **16**, 309 (2017).

[34] J. M. Gomez-Perez, X.-P. Zhang, F. Calavalle, M. Ilyn, C. González-Orellana, M. Gobbi, C. Rogero, A. Chuvilin, V. N. Golovach, L. E. Hueso, F. S. Bergeret, and F. Casanova, Strong interfacial exchange field in a heavy metal/ferromagnetic insulator system determined by spin Hall magnetoresistance, Nano Lett. **20**, 6815 (2020).

[35] N. Vlietstra, J. Shan, V. Castel, J. Ben Youssef, G. E. W. Bauer, and B. J. van Wees, Exchange magnetic field torques in YIG/Pt bilayers observed by the spin-Hall magnetoresistance, Appl. Phys. Lett. **103**, 032401 (2013).

[36] S. Nakatsuji, N. Kiyohara, and T. Higo, Large anomalous Hall effect in a non-collinear antiferromagnet at room temperature, Nature (London) **527**, 212 (2015).

[37] X. Chen, T. Higo, K. Tanaka, T. Nomoto, H. Tsai, H. Idzuchi, M. Shiga, S. Sakamoto, R. Ando, H. Kosaki, T. Matsuo, D. Nishio-Hamane, R. Arita, S. Miwa, and S. Nakatsuji, Octupole-driven magnetoresistance in an antiferromagnetic tunnel junction, Nature (London) **613**, 490 (2023).

[38] J. Han, T. Uchimura, Y. Araki, J.-Y. Yoon, Y. Takeuchi, Y. Yamane, S. Kanai, J. Ieda, H. Ohno, and S. Fukami, Room-temperature flexible manipulation of the quantum-metric structure in a topological chiral antiferromagnet, Nat. Phys. **20**, 1110 (2024).

[39] J.-Y. Yoon, P. Zhang, C.-T. Chou, Y. Takeuchi, T. Uchimura, J. T. Hou, J. Han, S. Kanai, H. Ohno, S. Fukami, and L. Liu, Handedness anomaly in a non-collinear antiferromagnet under spin–orbit torque, Nat. Mater. **22**, 1106 (2023).

[40] J. Yoon, Y. Takeuchi, R. Itoh, S. Kanai, S. Fukami, and H. Ohno, Crystal orientation and anomalous Hall effect of sputter-deposited non-collinear antiferromagnetic Mn_3Sn thin films, Appl. Phys. Express **13**, 013001 (2020).

[41] See Supplemental Material at http://link.aps.org/supplemental/10.1103/PhysRevLett.134.096701 for additional measurements and detailed theory, which includes Refs. [42–48].

[42] D. T. Son and B. Z. Spivak, Chiral anomaly and classical negative magnetoresistance of Weyl metals, Phys. Rev. B **88**, 104412 (2013).

[43] S. Meyer, M. Althammer, S. Geprägs, M. Opel, R. Gross, and S. T. B. Goennenwein, Temperature dependent spin transport properties of platinum inferred from spin Hall magnetoresistance measurements, Appl. Phys. Lett. **104**, 242411 (2014).

[44] T. Higo, D. Qu, Y. Li, C. L. Chien, Y. Otani, and S. Nakatsuji, Anomalous Hall effect in thin films of the Weyl antiferromagnet Mn_3Sn, Appl. Phys. Lett. **113**, 202402 (2018).

[45] J. M. Taylor, A. Markou, E. Lesne, P. K. Sivakumar, C. Luo, F. Radu, P. Werner, C. Felser, and S. S. P. Parkin, Anomalous and topological Hall effects in epitaxial thin films of the noncollinear antiferromagnet Mn_3Sn, Phys. Rev. B **101**, 094404 (2020).

[46] J.-Y. Yoon, Y. Takeuchi, S. DuttaGupta, Y. Yamane, S. Kanai, J. Ieda, H. Ohno, and S. Fukami, Correlation of anomalous Hall effect with structural parameters and magnetic ordering in $Mn_{3+x}Sn_{1-x}$ thin films, AIP Adv. **11**, 065318 (2021).

[47] K. Kuroda *et al.*, Evidence for magnetic Weyl fermions in a correlated metal, Nat. Mater. **16**, 1090 (2017).

[48] B. K. Hazra, B. Pal, J.-C. Jeon, R. R. Neumann, B. Göbel, B. Grover, H. Deniz, A. Styervoyedov, H. Meyerheim, I. Mertig, S.-H. Yang, and S. S. P. Parkin, Generation of out-of-plane polarized spin current by spin swapping, Nat. Commun. **14**, 4549 (2023).

[49] M. Althammer *et al.*, Quantitative study of the spin Hall magnetoresistance in ferromagnetic insulator/normal metal hybrids, Phys. Rev. B **87**, 224401 (2013).

[50] J.-J. Liu, K.-K. Meng, J.-K. Chen, Y. Wu, J. Miao, X.-G. Xu, and Y. Jiang, Robust interface-induced unusual anomalous Hall effect in Mn_3Sn/Pt bilayers, Rare Met. Cement. Carbides **41**, 3012 (2022).

[51] J. J. Liu, K. K. Meng, J. Q. Guo, Y. Wu, J. K. Chen, X. G. Xu, L. P. Sun, Y. Y. Han, and Y. Jiang, Giant interfacial spin-orbit scattering contribution to spin transport in Mn_3Sn/Pt bilayers, Phys. Rev. B **108**, 224406 (2023).

[52] Y. M. Lu, Y. Choi, C. M. Ortega, X. M. Cheng, J. W. Cai, S. Y. Huang, L. Sun, and C. L. Chien, Pt magnetic polarization on $Y_3Fe_5O_{12}$ and magnetotransport characteristics, Phys. Rev. Lett. **110**, 147207 (2013).

[53] T. Lin, C. Tang, H. M. Alyahayaei, and J. Shi, Experimental investigation of the nature of the magnetoresistance effects in Pd-YIG hybrid structures, Phys. Rev. Lett. **113**, 037203 (2014).

[54] Y. Yamane, O. Gomonay, and J. Sinova, Dynamics of noncollinear antiferromagnetic textures driven by spin current injection, Phys. Rev. B **100**, 054415 (2019).

[55] M. D. Stiles and A. Zangwill, Anatomy of spin-transfer torque, Phys. Rev. B **66**, 0144071 (2002).

[56] L. Baldrati, A. Ross, T. Niizeki, C. Schneider, R. Ramos, J. Cramer, O. Gomonay, M. Filianina, T. Savchenko, D. Heinze, A. Kleibert, E. Saitoh, J. Sinova, and M. Kläui, Full angular dependence of the spin Hall and ordinary magnetoresistance in epitaxial antiferromagnetic NiO(001)/Pt thin films, Phys. Rev. B **98**, 024422 (2018).

[57] K. Oyanagi, J. M. Gomez-Perez, X.-P. Zhang, T. Kikkawa, Y. Chen, E. Sagasta, A. Chuvilin, L. E. Hueso, V. N. Golovach, F. S. Bergeret, F. Casanova, and E. Saitoh, Paramagnetic spin Hall magnetoresistance, Phys. Rev. B **104**, 134428 (2021).

[58] A. Brataas, G. E. W. Bauer, and P. J. Kelly, Non-collinear magnetoelectronics, Phys. Rep. **427**, 157 (2006).